RF Pulses Modelization for EMG Signal Denoising in fRMI Environment

Sofia Ben Jebara
Carthage University, Ecole Supérieure des Communications de Tunis,
COSIM Laboratory,
Route de Raoued 3.5 Km, Cité El Ghazala, Ariana, 2088, Tunisia

Keywords: EMG Signal, fRMI, RF Pulses, HNM Model, Noise Reduction.

Abstract: This paper deals with noise contaminating EMG signal acquired in fRMI environment. The RF pulses are particularly addressed. Their characterization in the frequency domain allows their presentation as discrete pulses repeated at frequencies multiple of RF pulses repetition. The Harmonic plus Noise Model (HNM) is then used to model these pulses in the time-domain. The parameters of the model are extracted, frame by frame, according to the principle of short time analysis. The model is validated according to two criteria: the Segmental Signal to Noise Ratio (*SSNR*) and its Normalized Standard Deviation (NSD_{SSNR}). Once modeled, the estimated noise is subtracted from noisy observation of EMG signal, leading to an enhanced version. Simulation results are given, validating the approach. In absence of ground truth, realistic situations are simulated in order to calculate quantitative criteria. Furthermore, qualitative appreciation is given thanks to muscular contractions profiles. Finally, the results are compared to those obtained with spectral subtraction and comb filtering.

1 INTRODUCTION

The acquisition of EMG signals simultaneously with brain images in functional Magnetic Resonance Imaging (fRMI) environment offers an added value compared to acquisition of EMG signal outside the scanner. In fact, the combination of the two modalities allows to explore the dynamics of neural activity and to link it to muscle response to the brain command. However, these advantages come with drawbacks like artifacts: EMG data collected during fRMI experiments are contaminated by artifacts due to technical and physiological origins. The cross talk (electrodes over an adjacent muscle pick-up a signal via skin conduction) is one common physiological artefact, the EMG signal acquisition system (driver amplifier, electrodes, cable movement,...) is one source of technical artifact. In fRMI environment, the EMG signal is affected by a supplementary noise which has a very high level. It has two main origins: the very high static magnetic field (of the order of Tesla, which corresponds to thousands of times the earth's magnetic field) and the ordered combination of RF and gradient pulses designed to acquire the data to form the image. The radio frequency pulses are emitted to excite hydrogen nuclei for images generating while magnetic field gradients are introduced for spatial encoding of the image (see for example (Hornak, 2006) for more details).

Fig. 1 shows an example of EMG data acquired in normal conditions (outside the scanner) and in fRMI environment (inside the scanner). Segment 'Noise out' (resp. 'Noise in") corresponds to physiological and technical noises (resp. physiological, technical and specific fRMI noises) since there is no muscle activity and the acquisition is carried outside (resp. inside) the scanner. Segment 'EMG out' (resp. 'EMG in') corresponds to effective EMG signal during muscle activity outside (resp. inside) the scanner. One can notice the high level of noise due to radio-frequency and gradient pulses. This noise completely buries the EMG signal.

This paper aims at modelizing the RF pulses in order to denoise EMG signals acquired in fRMI environment. At the best of our knowledge, the mathematical modelization of fRMI noise did not attract the attention of researchers, even though it is well analyzed from a physical point of view and its origin and frequency properties are well mastered (see for example (Hoffmann et al., 2000)(Ganesh et al., 2007)(El Tatar, 2013)(Dougherty, 2010)(Garreffa et al., 2003)). In this paper, we propose to develop an analytical model of the RF pulses from observations when no prior information about RF pulses is available. The model

Ben Jebara, S.
RF Pulses Modelization for EMG Signal Denoising in fRMI Environment.
DOI: 10.5220/0007256401090115
In *Proceedings of the 12th International Joint Conference on Biomedical Engineering Systems and Technologies (BIOSTEC 2019)*, pages 109-115
ISBN: 978-989-758-353-7

takes its origin from spectral characterization of noise and leads to an Harmonic plus Noise Model (HNM). This model will be exploited to denoise EMG signal acquired in RMI environment.

The paper is organized as follows. Section 2 describes the RF noise in temporal and frequency domains. Section 3 is devoted to HNM model explanation and the algorithm to calculate its parameters. Section 4 takes advantage of the model to reduce noise from the EMG signal. Section 5 compares the performances of proposed HNM model to Comb filtering and Spectral Subtraction technique. Finally, conclusions are drawn.

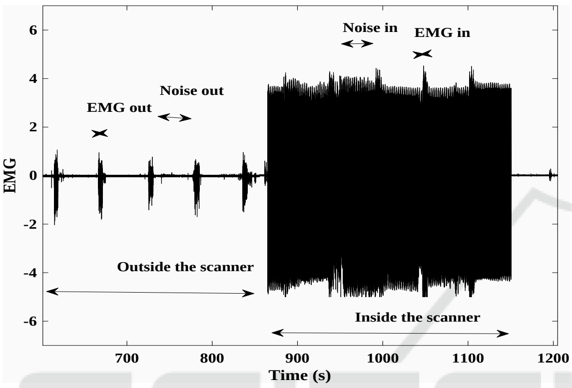

Figure 1: Temporal evolution of EMG signal before and during image acquisition in fRMI tunel.

2 RF NOISE PROPERTIES

2.1 Data Acquisition

Participants were lying in the fRMI scanner with forearm connected to bipolar electrodes (ADD208, 8-mm recording diameter, System Inc., Santa Barbara, CA). Surface EMG signals were recorded during a handgrip exercice from the Flexor Digitorum Superficialis (FDS) muscle. Simultaneously, neuro-imaging data were acquired with an MRI system. The RF pulses and the gradient fields are applied repetitively to acquire image slices of the brain. One loop, for complete brain volume scan, occurs during a time interval called repetition time (denoted T_R). One loop allows to generate a sequence of images (slices). Each image is obtained during one RF stimulation period. The duration between two RF pulses T_0 is equal to the repetition time T_R over the number of slices N: $T_0 = T_R/N$.

2.2 RF Pulses Properties

To study the influence of the noise generated by RF pulses in the EMG signal, let's consider some examples of RF pulses commonly used in practice. Fig. 2 gives time-continous temporal evolution (a) and spectrums (b) of some common RF pulses, namely rectangle, windowed sinus cardinal, Gaussian and Fermi (Bernstein et al., 2004). Note that only the active part (non null part) is drawn and figures axis are not given in order to focus only on the shape. All the pulses are time-limited. In the frequency domain, the Gaussian, the windowed sinus cardinal and Fermi pulses are characterized by band-limited spectrum while rectangular pulse is characterized by an infinite frequency support.

The RF pulses are repeated periodically in order to acquire the whole image slices of the brain. Let's denote $x(t)$ the RF pulse. According to its periodicity property, its Fourier transform is a sum of dirac pulses equally spaced in the frequency axis at frequencies multiple of f_0:

$$\mathbf{X}(f) = \sum_{k \in Z} \mathbf{X}_k \delta(f - kf_0), \tag{1}$$

where $\mathbf{X}_k$ is the k^{th} Fourier transform coefficient, calculated during one period according to the following formula:

$$\mathbf{X}_k = \frac{1}{T_0} \int_{\frac{-T_0}{2}}^{\frac{T_0}{2}} x(t) e^{-j2\pi \frac{k}{T_0} t} dt. \tag{2}$$

The RF analog signal is converted to a digital one. When sampled and according to Shannon theorem, a spectral overlap can appears due to the duplication of the spectrum around the multiples of the sample frequency:

$$\mathbf{Xs}(f) \stackrel{\triangle}{=} f_s \sum_{l \in Z} \mathbf{X}(f - lf_s) = f_s \sum_{k \in Z} \sum_{l \in Z} \mathbf{X}_k \delta(f - lf_s - kf_0). \tag{3}$$

With an appropriate choice of the parameters of the RF pulse, their bandwidth can be adjusted so that the duplication of spectrum around sampling frequency multiples allows to reduce/avoid overlapping. While windowed sinus cardinal, Gaussian and Fermi RF pulses can lead to non-overlapping (thanks to their band-limited spectrum), the rectangle pulse generates overlapping (because of its infinite frequency support). An alternative solution is to increase the sampling frequency so that the overlap becomes less important (since the secondary lobes vanish when the frequency increases). But increasing the sampling frequency increases the number of samples acquired, which is not necessarily interesting in term of data amount.

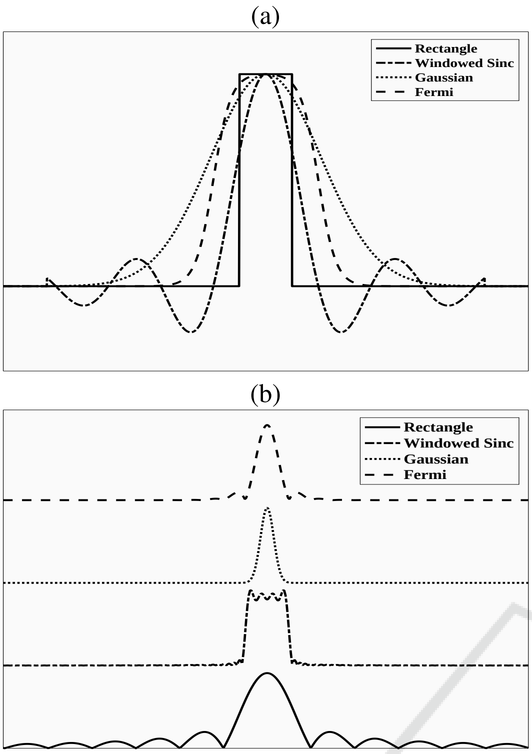

Figure 2: Some common RF pulses. Spectrums are shifted for better legibility.

2.3 RF Pulses Properties as Noise in EMG

To deal with a concrete example, we consider the case where the repetition time is equal to $T_R = 2215\,\text{ms}$ and $N = 43$ images are acquired. The frequency of repetition of RF pulses is $f_0 = 1/T_0 = 9.706\,\text{Hz}$. The signal of interest is the EMG signal of FDS muscle. Its maximum frequency is 500 Hz so that it should be ideally sampled at 1 kHz. The RF interference acquired as noise in EMG is sampled at the same frequency.

Fig. 3 shows the spectrum of noise generated during real acquisition in the RMI tunnel (according to the protocol described in subsection 2.1). Note that frequency bins due to RF noise exist along the whole frequency axis at frequencies multiple of $f_0 = 9.706\,\text{Hz}$. Their amplitudes differ from one frequency to another. This noise spectrum is compared to the one of an EMG signal which looks like a white noise with relatively very low level compared to that of RF pulses. Hence, the challenging task is to estimate this noise and to reduce it.

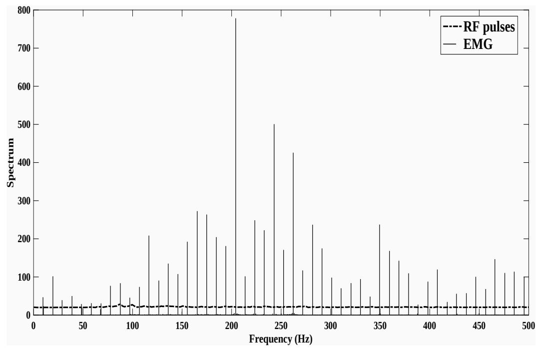

Figure 3: Spectrum of EMG signal and noise generated during a real acquisition in the RMI tunnel.

3 RF PULSES MODELISATION

Eq. 3 describes digital RF pulses as a weighted sum of frequency bins. Hence, in time-domain, we propose to model the periodic RF pulses as a weighted sum of sine waves:

$$\tilde{x}(m) = \sum_{k=0}^{K-1} a_k(m) \sin\left(2\pi k \nu_0 m + \phi_k(m)\right), \quad (4)$$

where $\tilde{x}(m)$ is the modeled sample at time index m, K is the number of harmonics. For each harmonic k, $a_k(m)$ and $\phi_k(m)$ represent the time-varying amplitude and phase respectively. ν_0 is the normalized frequency $\nu_0 = \frac{f_0}{f_s}$. The number of harmonics is equal to the nearest integer of the signal maximal frequency $(fs/2)$ over the fundamental frequency f_0:

$$K = \lfloor \frac{fs}{2f_0} \rfloor. \quad (5)$$

For our practical case, the EMG signal is sampled at $f_s = 1$ kHz and RF fundamental frequency is $f_0 = 9.706$, so the number of harmonics is $K = 51$.

3.1 Model Parameters Calculs

To estimate the parameters of the model, the following methodology is adopted. It is inspired from previous works developed on speech processing (see for example (Pantazis, 2010)).

- In the RMI tunnel, the RF pulses generator is turned on. EMG signals acquisition are placed on the considered muscle and the subject is asked to not do any muscular activity. The EMG acquisition system is turned on so that the acquired signal is the environmental noise. It is composed of technical and physiological artefacts, static magnetic field, RF pulses and gradient fields.

- Short-term analysis is done. The recorded signal is decomposed into frames of length N and is windowed using Hanning window for example. The frame by frame analysis allows to assume that amplitudes and phases of the harmonics are constant within a frame. The choice of the frame size will be discussed later.
  Let's denote $x_l(u)$ the u^{th} sample $(u = 0, ..N-1)$ belonging to the frame number l of the signal.
- The frequency f_0 of RF pulses could be known from the RMI scanner datasheet. Otherwise, it can be estimated using any precise method of periodicity measure or by spectrum peak picking. The estimated normalized frequency is denoted $\widehat{\nu}_0$.
- Each frame is converted to the analytic complex signal using the Hilbert transform. It is denoted $x_l^H(u)$.
- The estimation of the amplitudes $a_{k,l}$ and the phases $\phi_{k,l}$ of each harmonic k, for each frame l is performed by minimizing the Least Squared (LS) error between the Hilbert transformed signal $x_l^H(u)$ and the Hilbert transformed modeled RF noise $\widehat{x}_l^H(u)$:
  $$\begin{aligned} e_l(u) &= x_l^H(u) - \widehat{x}_l^H(u) \\ &= x_l^H(u) - \sum_{k=0}^{K-1} \widehat{a}_{k,l} e^{j\left(2\pi k \widehat{\nu}_0 u + \widehat{\phi}_{k,l}\right)} \end{aligned} \quad . \qquad (6)$$
  where $\widehat{a}_{k,l}$ and $\widehat{\phi}_{k,l}$ are the parameters to be determined.
- Minimizing the Least Square error leads to the following solution:
  $$\widehat{V}_l = (M^T W^T W M)^{-1} M^T W^T W X_l^H, \qquad (7)$$
  where T is the transpose operator, $X_l^H = [x_l^H(0), x_l^H(1), ..., x_l^H(N-1)]^T$ is the vector of Hilbert transformed samples, W is the analyzing window vector of length N, M is a matrix of dimension $N \times K$ containing the exponential terms $M(l,k) = e^{j2\pi\widehat{\nu}_0 kl}$. $\widehat{V}_l = [\widehat{v}_{0,l}, \widehat{v}_{1,l}, ..., \widehat{v}_{K-1,l}]^T$ is the unknown vector of parameters.
  One term $\widehat{v}_{k,l}$ is written:
  $$\widehat{v}_{k,l} = \widehat{a}_{k,l} \cos\left(\widehat{\phi}_{k,l}\right) - j\widehat{a}_{k,l} \sin\left(\widehat{\phi}_{k,l}\right). \qquad (8)$$
  The final solution is $\widehat{a}_{k,l}$ extracted as the modulus of $\widehat{v}_{k,l}$ and $\widehat{\phi}_{k,l}$ which is its phase.
- Once the parameters estimated, the RF pulse frame is written:
  $$\widehat{x}_l(u) = \sum_{k=0}^{K-1} \widehat{a}_{k,l} \cos\left(2\pi k \widehat{\nu}_0 l + \widehat{\phi}_{k,l}\right). \qquad (9)$$
- The whole estimated signal $\widehat{x}(m)$ is estimated by concatenating estimated frames.

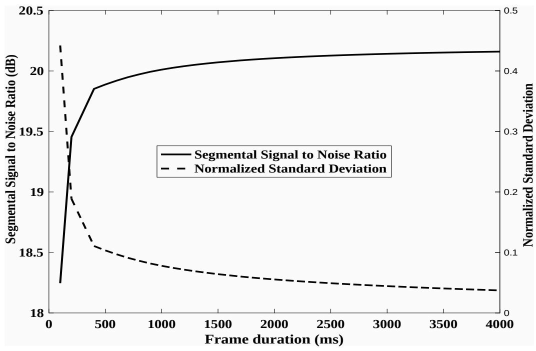

Figure 4: Segmental Signal to Noise Ratio and Normalized Standard Deviation versus frame length.

3.2 Frame Size Choice

The choice of frame size is crucial to obtain good RF pulse modelization. Two criteria are used to quantify the performances: the Segmental Signal to Noise Ratio ($SSNR$) which is the mean value of the SNR (in dB) calculated for each frame and its Normalized Standard Deviation (NSD_{SSNR}), useful to put into proportion the $SSNR$ deviation along frames compared to its mean. The two criteria are defined as follows:

$$SSNR = \frac{1}{M} \sum_{l=1}^{M} 10 \log 10 \left(\frac{\sum_{u=1}^{N} x_l(u)^2}{\sum_{u=1}^{N} [x_l(u) - \widehat{x}_l(u)]^2} \right), \qquad (10)$$

and

$$NSD_{SSNR} = \frac{\sigma_{SSNR}}{m_{SSNR}}, \qquad (11)$$

where σ_{SSNR} (resp. m_{SSNR}) is the $SSNR$ standard deviation (resp. mean) and M is the total number of frames. Fig. 4 plots the evolution of both criteria for different frame lengths. One can see that $SSNR$ increases and NSD_{SSNR} decreases when frame length increases. It means that better modelisation is obtained for longer frames. However, the rate of improvement begins to stabilize around a frame size of one second. This duration is considered adequate for this study.

4 INTEREST IN EMG SIGNAL DENOISING

4.1 The Idea

One RF pulse modelled, it is possible to reduce its effect on acquired EMG signal when RMI scanning is turned on and when the subject is activating its muscle and doing the requested muscular exercice. The corrupted EMG signal $y(m)$ can be presented as the sum of the muscle signal $emg(m)$, the RF signal $x(m)$ and any other additive noises $n(m)$:

$$y(m) = emg(m) + x(m) + n(m). \tag{12}$$

The enhanced emg signal should be simply obtained by subtracting the modeled RF signal $\widehat{s}(m)$ from the observation $y(m)$:

$$\widehat{emg}(m) = y(m) - \widehat{x}(m). \tag{13}$$

Note that other additive noises are not yet considered during this step, because of their low level compared to that of RF noise. Common technical artifacts can be reduced, in a post processing stage, using other approaches (see for example (Thakor and Zhu, 1991) for reducing power line electrical noise, (Lu et al., 2009) to suppress electrocardiogram (ECG) interference, (De Luca et al., 2010) to remove noise associated to mechanical perturbations...).

4.2 Illustration

When acquired, the EMG signal is buried in noise and there is no ground truth to quantitatively measure the performance. The idea developed here is to compare the signal with a reference which could be the signal acquired out of scanner. Hence, the same participant is asked to do the same handgrip exercice inside and outside scanner according to the same experimental paradigm. In each case, he did 15 contractions of duration 4.4 seconds approximatively, separated by a rest time of 44 seconds.

Fig. 5 (resp. Fig. 6) shows the temporal evolution (resp. spectrogram) of an EMG signal acquired in the fRMI environment described previously, the denoised one using the proposed approach and the acquired EMG outside the scanner (called the reference). One can notice that EMG signal emerges from noise despite the presence of small residual noise, and the contractions have the same aspect as the ones of the reference.

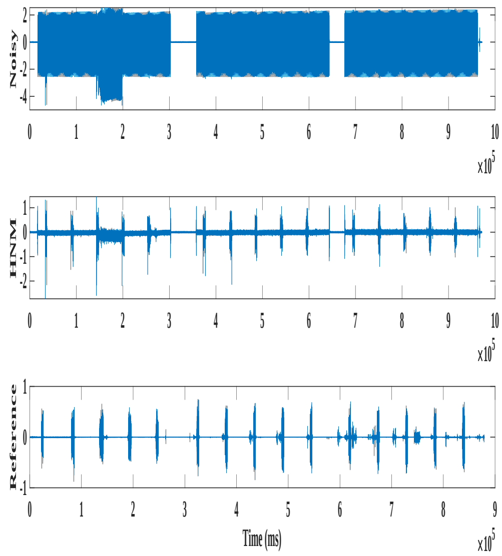

Figure 5: Temporal evolution of noisy, denoised and reference EMG signals.

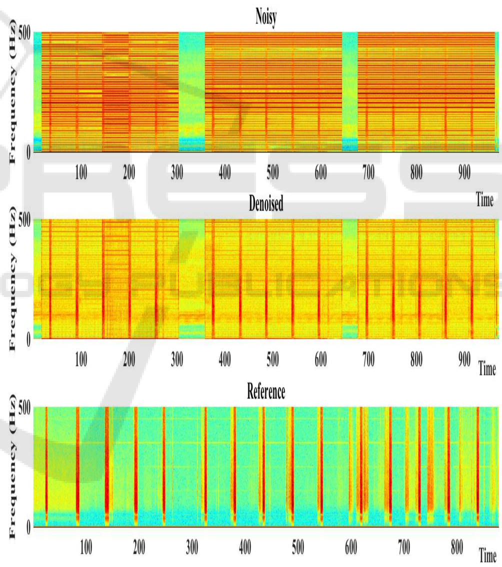

Figure 6: Spectrograms of noisy, denoised and reference EMG signals.

5 PERFORMANCES AND COMPARISON

5.1 Overview on Comb Filtering and Spectral Subtraction Methods

According to the state of art, few methods are developed to extract RF pulses from physiological signals acquired in RMI tunnel. The most common approach is based on Comb filtering (see for example (Ganesh et al., 2007)). It operates in the temporal domain and makes use of a digital filter which cancels frequency components situated at frequencies multiple of fundamental frequency of RF pulses while keeping intact the other frequencies.

Another approach is based on spectral subtraction (see for example (Ben Jebara, 2014)). It operates in the frequency domain to estimate the noise spectrum and to subtract it from noisy observation spectrum. The noise estimation is based on spectral minima tracking in each frequency bin without any distinction between muscle activity and muscle rest. But it looks for connected time-frequency regions of muscle activity presence to estimate a bias compensation factor. The proposed approach denoted HNM (Harmonic plus Noise Model) is compared to spectral subtraction and Comb filtering.

5.2 Comparison Criteria

To compare the methods, two criteria are used. The first one is quantitative and has the form of Mean Signal To Noise Ratio (*MSNR*) while the second one is qualitative and uses the contraction profile.

- The *MSNR* is calculated as a mean value of 285 *SNR* values obtained by studying FDS muscle contractions made by 19 subjects, each repeating the action 15 times. One *SNR* is calculated by taking data from a clean EMG signal acquired outside the tunnel. An additive real fRMI noise, acquired in fRMI tunnel without exercing any contraction, was added by varying its level (artificial attenuation and amplification). Thus, it is possible to calculate noisy *MSNR* (denoted $MSNR_{Noisy}$) and one *MSNR* at the output of the denoiser (denoted $MSNR_{Denoised}$).
- The contraction profile is a visual criteria used to evaluate the quality of denoising. It is obtained thanks to the Root Mean Square signal which is a technique for rectifying the raw signal and converting it to an amplitude envelope. It is defined as follows:

$$RMS(m) = \sqrt{\frac{1}{N}\sum_{n=-N/2}^{N/2-1} x(m+n)^2}, \qquad (14)$$

  where $x(n)$ is the m^{th} sample of the signal on interest and L is the length of the rectifying window. It is chosen equal to $L = 512$ for a sampling frequency of $f_s = 1\,\text{kHz}$.

5.3 Results

Fig. 7 shows the evolution $MSNR_{Denoised}$ for different values of $MSNR_{Noisy}$ ranging from -16 dB to 10 dB dB. One can notice that, unlike HNM whose performances vary according to the level of noise, Comb filtering and spectral subtraction lead to quasi-constant values of $MSNR_{Denoised}$, independently of the noise level. Furthermore, Comb filtering and spectral subtraction give better $MSNR_{Denoised}$ for high level of noise ($MSNR_{Noisy} <$ -7 dB) while HNM performs for greater values of $MSNR_{Noisy}$.

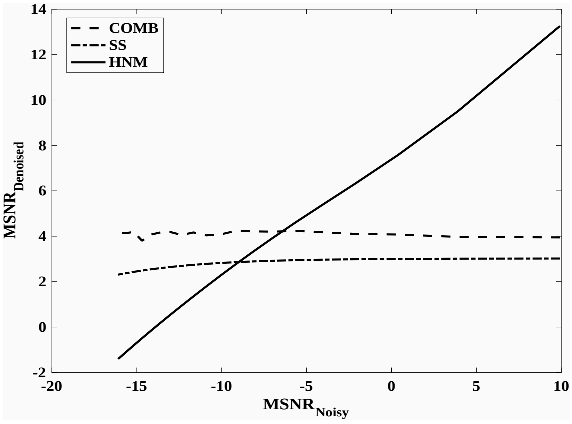

Figure 7: Evolution of $MSNR_{Denoised}$ versus $MSNR_{Noisy}$.

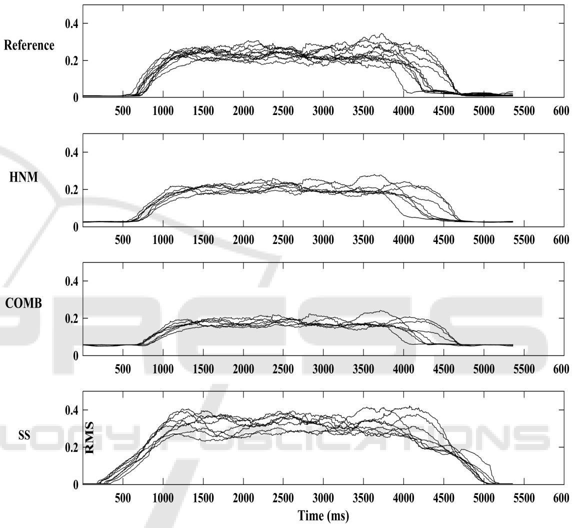

Figure 8: Contractions profile.

If we consider a real acquisition system: Biopac MP150 system to digitize EMG data and General Electric Medical System 3-Tesla whole-body MRI system to generate RF pulses, a typical value of $MSNR_{Noisy}$ is in the range $[0\;1]\;dB$. In such case, HNM should be used.

Fig. 8 draws the contraction profiles for the reference signal acquired outside the scanner and the ones obtained after denoising. It is important to notice that the contraction durations are not exactly the same even though the volunteers were asked the follow the same paradigm. The contraction durations are artificially contracted/expanded in time so that comparison is confortable. Fig. 8 shows that contractions profiles are well restored. Their level is attenuated with comb filtering, their duration (at the beginning and at the end) is extended with spectral subtraction. It seems that HNM gives the best profile.

6 CONCLUSION

In this paper, the problem of RF pulses noise contaminating the EMG signal acquired in fRMI scanner is addressed. Thanks to its description in the frequency domain and to its modelization using Harmonic plus Noise model, it was possible to subtract it from EMG signal, rmaking it exploitable for further analysis and processing.

ACKNOWLEDGEMENTS

The authors are thankful to the team 'Biomechanics, Imagery and Physiology Movement Analysis' of Movement and Sport Research Centre (CeRSM) at Paris 10 University, for asking the resolve the problem of EMG enhancement and providing the experimental data.

REFERENCES

Ben Jebara, S. (2014). Electromyogram signal enhancement in frmi noise using spectral subtraction. In *Proceedings of the 22nd European Signal Processing Conference*, pages 1980–1984.

Bernstein, M. A., King, K. F., and Zhou, X. J. (2004). *Handbook of MRI pulse sequences*. Elsevier.

De Luca, C. J., Gilmore, L. D., Kuznetsov, M., and Roy, S. H. (2010). Filtering the surface emg signal: Movement artifact and baseline noise contamination. *Journal of biomechanics*, 43(8):1573–1579.

Dougherty, J. B. (2010). *A novel and comprehensive artifact reduction strategy for EMG collected during fMRI at 3 Tesla*. PhD thesis, Drexel University.

El Tatar, A. (2013). *Caractérisation et modélisation des potentiels induits par les commutations des gradients de champ magnétique sur les signaux électrophysiologiques en IRM*. PhD thesis, Université de Technologie de Compiègne.

Ganesh, G., Franklin, D. W., Gassert, R., Imamizu, H., and Kawato, M. (2007). Accurate real-time feedback of surface emg during fmri. *Journal of neurophysiology*, 97(1):912–920.

Garreffa, G., Carnı, M., Gualniera, G., Ricci, G., Bozzao, L., De Carli, D., Morasso, P., Pantano, P., Colonnese, C., Roma, V., et al. (2003). Real-time mr artifacts filtering during continuous eeg/fmri acquisition. *Magnetic resonance imaging*, 21(10):1175–1189.

Hoffmann, A., Jäger, L., Werhahn, K., Jaschke, M., Noachtar, S., and Reiser, M. (2000). Electroencephalography during functional echo-planar imaging: detection of epileptic spikes using post-processing methods. *Magnetic Resonance in Medicine: An Official Journal of the International Society for Magnetic Resonance in Medicine*, 44(5):791–798.

Hornak, J. P. (2006). The basics of mri. *http://www. cis. rit. edu/htbooks/mri*.

Lu, G., Brittain, J. S., Holland, P., Yianni, J., Green, A. L., Stein, J. F., and Wang, S. (2009). Removing ecg noise from surface emg signals using adaptative filtering. *Neuroscience letters*, 462(1):14–19.

Pantazis, Y. (2010). *Decomposition of AM-FM signals with applications in speech processing*. PhD thesis, University of Crete.

Thakor, N. V. and Zhu, Y.-S. (1991). Applications of adaptive filtering to ecg analysis: noise cancellation and arrhythmia detection. *IEEE Transactions on biomedical engineering*, 38(8):785–794.